Environmental Science & Technology

RETURN TO ISSUE

< PREV ECOTOXICOLOGY AND PU... NEXT >

Environmental Science & Technology Get e-Alerts

Stability of Aerosolized SARS-CoV-2 on Masks and Transfer to Skin

Jin Pan, Selma Gmati, Bryce A. Roper, Aaron J. Prussin II, Seth A. Hawks, Abby R. Whittington, Nisha K. Duggal, and Linsey C. Marr*

Cite this: *Environ. Sci. Technol.* 2023, 57, 28, 10193–10200
Publication Date: July 3, 2023
https://doi.org/10.1021/acs.est.3c01581
Copyright © 2023 The Authors. Published by American Chemical Society. This publication is licensed under CC-BY-NC-ND 4.0.
Open Access

Article Views 721 | Altmetric 536 | Citations 2
LEARN ABOUT THESE METRICS

Share Add to Export RIS

PDF (2 MB)

SI Supporting Info (1) »

SUBJECTS: Anatomy, Infectious diseases,

Abstract

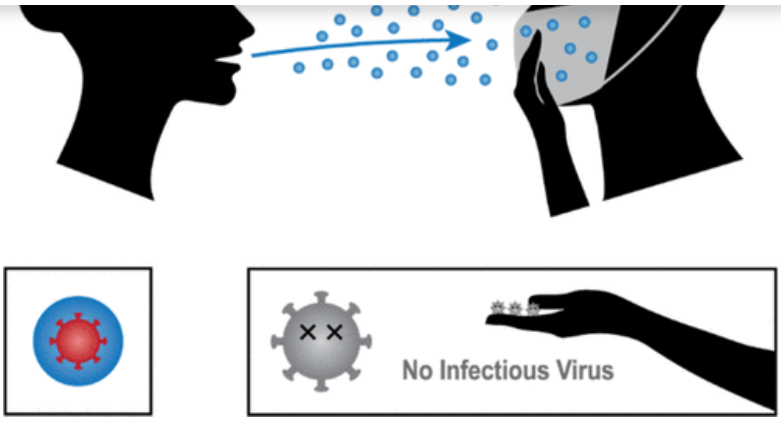

The potential for masks to act as fomites in the transmission of SARS-CoV-2 has been suggested but not demonstrated experimentally or observationally. In this study, we aerosolized a suspension of SARS-CoV-2 in saliva and used a vacuum pump to pull the aerosol through six different types of masks. After 1 h at 28 °C and 80% RH, SARS-CoV-2 infectivity was not detectable on an N95 and surgical mask, was reduced by 0.7 $\log_{10}$ on a nylon/spandex mask, and was unchanged on a polyester mask and two different cotton masks when recovered by elution in a buffer. SARS-CoV-2 RNA remained stable for 1 h on all masks. We pressed artificial skin against the contaminated masks and detected the transfer of viral RNA but no infectious virus to the skin. The potential for masks contaminated with SARS-CoV-2 in aerosols to act as fomites appears to be less than indicated by studies involving SARS-CoV-2 in very large droplets.

This publication is licensed under CC-BY-NC-ND 4.0.

KEYWORDS: SARS-CoV-2, aerosol, survival, mask

Synopsis

Aerosolized SARS-CoV-2 survives on some masks, but only viral RNA and not infectious virus is transferred from contaminated masks to skin.

Introduction

Jump To

Widespread masking during the Covid-19 pandemic has renewed questions about the

Environmental Science & Technology

processes in this route are the ability of the virus to survive on a surface and the efficiency of its transfer from the surface to people's hands. Previous studies have assessed the survival of SARS-CoV-2 in droplets on different surfaces, including plastics, metals, textiles, and personal protective equipment. (8−15)

In studies of the stability of SARS-CoV-2 on textiles, researchers typically apply 5−50 μL of virus in culture medium to the surface, incubate the material under specific environmental conditions, and then attempt to recover the virus. SARS-CoV-2 lost infectivity on cotton after 4 h in one study, (10) whereas it remained detectable for several days in others. (11,12,15) The virus persisted on polyester-containing materials for a few hours, (14,15) and on surgical masks for 4−7 days. (8,11) Virus infectivity on textiles varies with temperature and RH. On N95 respirators, SARS-CoV-2 persisted for 2 days at 25 °C and 70% RH (13) and up to 21 days at cooler and drier conditions of 20 °C and 35−40%. (10) A similar relationship with temperature and RH was also found on Tyvek. (10,13,15) Additional details about the initial droplet size, starting titer, media, temperature, RH, and results in these studies are listed in Table S1. In summary, prior studies have shown that SARS-CoV-2 in large droplets remains infectious for the longest period on N95s, followed by surgical masks, cotton, and polyester, and that virus viability is sensitive to temperature and RH.

These studies address fomite transmission involving large droplets that have deposited on the inside or outside of a mask, but they may not adequately capture the risk of transmission via much smaller aerosol particles that have deposited on the mask. In terms of number, over 90% of respiratory particles released during talking and coughing are <20 μm. The largest of these is 4×10^{-6} μL in volume, (16,17) many orders of magnitude smaller than the droplets (>5 μL) used to mimic contaminated surfaces in previous studies. (8−15) SARS-CoV-2 has been shown to decay faster in smaller droplets compared to larger ones (1 vs 50 μL) under some conditions. (18) Therefore, it is essential to examine the survival of SARS-CoV-2 deposited on masks in aerosolized form.

In addition to evaluating the viability of aerosolized SARS-CoV-2 on masks, we must also consider the potential for viruses to be transferred to the skin. A recent study has demonstrated that up to 16% of nondried infectious SARS-CoV-2 can be successfully transferred from contaminated solids to artificial skin applied with a force of 3 N; however, it is reduced by 50−75% once dried. (19) Another study reported that an average of 17% of a model enveloped virus, the bacteriophage phi6, and 26% of a nonenveloped virus, MS2, transferred from solid surfaces (stainless steel, painted wood, and plastic) to fingerpads. (20) Data on the transfer of virus from textiles to skin are limited. One study found that the

Environmental Science & Technology

For fomite transmission to occur, the virus must not only be physically transferred to the skin, but it must also maintain infectivity. Previous studies have shown that SARS-CoV-2 in large droplets remains infectious on swine skin for 96 hours at 22 °C and 40–50% RH, (14) and on abdominal skin from autopsy for 4–8 h at 25 °C and 45–55% RH. (22) However, whether aerosolized SARS-CoV-2 can maintain infectivity after transfer from fabric to skin is still unknown.

The objective of this study is to assess the potential for fomite transmission of SARS-CoV-2 via contaminated masks. To simulate contamination of masks by inhalation of the virus from the surrounding air, we aerosolized SARS-CoV-2 and used a vacuum pump to pull the aerosol through six different types of masks. We chose to incubate the contaminated masks for 1 h to simulate the duration of a typical meeting or shopping excursion. Following incubation of the masks for 1 h, we eluted them and detected infectious virus on polyester, cotton knit, cotton poplin, and nylon/spandex masks but not on an N95 respirator and surgical mask. We pressed artificial skin against the masks and were able to recover SARS-CoV-2 RNA but not infectious virus from the skin. Finally, we assessed whether survival and transfer of the virus were associated with the surface roughness and hydrophobicity of the masks.

Methods and Materials

Jump To

Mask Preparation

We acquired six commercially available masks for testing. Table 1 lists the masks and their materials, and Figure S1 shows photos of them. Following the manufacturers' suggestion to wash before wearing, we machine-washed the four cloth masks for one regular cycle with detergent and one cycle without detergent (water only). We allowed them to air-dry. We found that washing was needed to remove chemical residuals that may inhibit downstream biological processes, such as plaque assay and qPCR. This step also affected the masks' physical properties. For all masks except the cotton poplin one, the surface roughness decreased after washing (Tables 2 and S2).

Table 1. Masks Tested in This Study

name	inner layer	middle layer	outer layer
N95 respirator	polyester	polypropylene	polyester

Environmental Science & Technology

polyester	cotton blend	cotton blend	100% polyester
cotton knit	100% cotton knit		
cotton poplin	100% cotton poplin		
nylon/spandex	90% nylon, 10% spandex	polypropylene	90% nylon, 10% spandex

Table 2. Physical Properties of Masks and Artificial Skin Tested in This Study[a]

name	surface roughness S_a (μm)	contact angle (°)	absorption time (s
N95 respirator	48 ± 15	N/A	21 ± 16
surgical mask	39 ± 20	91 ± 16	N/A
polyester	48 ± 20	103 ± 14	N/A
cotton knit	59 ± 9	N/A	38 ± 19
cotton poplin	22 ± 3	N/A	45 ± 9
nylon/spandex	43 ± 12	N/A	52 ± 17
artificial skin	39 ± 4.2	N/A	N/A

[a]Surface roughness (S_a) reported as arithmetic mean height. Contact angle provided for masks on which a droplet remained stable. Absorption time provided for masks on which a droplet was quickly absorbed. Values are presented as mean ± standard deviation.

Filtration Efficiency

To evaluate the masks' ability to collect aerosolized SARS-CoV-2, we measured their material filtration efficiency for particles of diameter 0.06–2 μm (Figure S3) using the same methods as in our prior study of masks, (23) with two differences. First, we used a medical nebulizer (AIRIAL) instead of a Collison nebulizer to generate aerosols. Second, to match the flow rate used to load masks with virus in the present study, we tested filtration efficiency at a flow rate

detailed description of the methods is provided in the Supporting Information (SI).

Mask Surface Roughness and Hydrophobicity

We characterized the surface roughness of the outer surface of each mask and its hydrophobicity using all layers of the mask held together and intact with metal fasteners. We cut 4–6 strips from each mask and flattened them for testing. We used a noncontacting profilometer (Keyence VK-X3000) to measure surface profiles, avoiding seams and printed markings. We mounted flattened samples to glass slides for profiling by a laser scanning confocal microscope. For all samples, micrographs were taken at 10× magnification. Once a focused and clear image was obtained, surface height was evaluated from the four quadrants of the image, each section being defined as 350 μm × 350 μm, and the arithmetical mean height (S_a) was measured. Results were then reported as the mean ± standard deviation.

We analyzed the hydrophobicity of the masks using a contact angle meter (Biolin Scientific Attension Theta Flow). We calibrated the tensiometer using a ball bearing with the camera angle set to 0°. A 200 μL pipette tip attached to the machine was filled with reverse osmosis water. We programmed the instrument to perform a sessile drop test using a 6–7 μL droplet applied to the sample. Images were recorded at 10 frames per second, and a contact angle was auto-calculated using Young–Laplace equations. Samples that absorbed the droplet were not assigned a contact angle; instead, an adsorption time was recorded. Absorption times were recorded from the initial contact on the droplet until it was visually fully absorbed by the material. Ten droplets per sample were measured for each mask type, and the results were reported as the mean ± standard deviation.

Virus Preparation

We passaged the SARS-CoV-2 strain USA-WA1/2020 (BEI Resources NR-52281) in Vero E6 cells once and subsequently in Vero cells once, as described in Hawks et al. (24) All experiments were conducted in a biosafety level 3 (BSL-3) laboratory. The initial titer of harvested viruses was 7 $\log_{10}$ PFU/mL. We further diluted the virus stock in pooled human saliva (Lot 33265, Innovative Research) to 5 $\log_{10}$ PFU/mL, which was used for SARS-CoV-2 aerosol generation.

Aerosol Generation and Mask Contamination

We evaluated the stability of SARS-CoV-2 aerosols on the masks in an induction chamber

nebulizer's cup with 1 mL of virus suspension in saliva. Three 25 mm stainless steel filter holders (Advantec LS25) were positioned inside the chamber, each connected to a high-efficiency particulate air filter capsule (TSI HEPA Grade, model 1602345) and a pump (SKC AirChek XR5000) located outside the chamber (Figure 1). Each pump ran at a flow rate of 2 L/min, resulting in a total flow rate of 6 L/min being removed from the chamber. This flow rate was chosen to achieve a balance between the nebulizing flow (5 L/min) and the sampling flow (6 L/min), with the latter slightly higher than the former to maintain negative pressure in the chamber. Make-up air entered the chamber through a 5 mm slit on the top, through the partially open lid, as shown in Figure 1. A sensor (HOBO UX100-011) inside the chamber monitored temperature and RH. A small fan was installed in front of the aerosol inlet to mix the air inside the chamber. The entire experiment was contained in a biosafety cabinet in a BSL-3 laboratory.

Figure 1

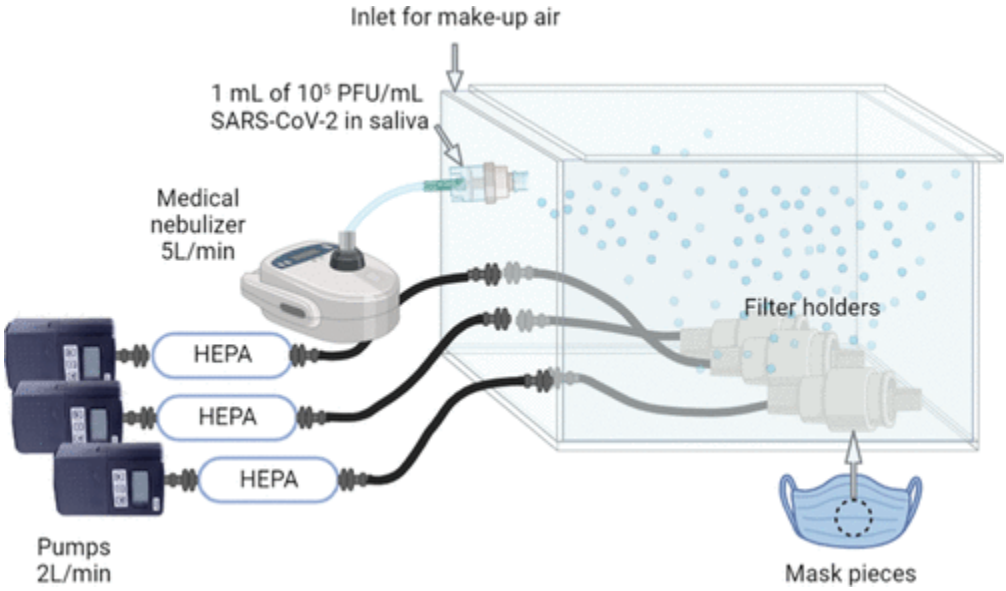

Figure 1. Schematic of the setup for aerosol generation and mask contamination. The figure was created using Biorender.com.

We ran an experiment to verify that the three filter holders experienced similar concentrations of particles. Using an optical particle counter (TSI AeroTrak 9306), we measured the particle concentration and size distribution through each filter holder. For biosafety reasons, we nebulized saliva alone, without virus, for this experiment (Figure S2). There were no significant differences among the three filter holders in terms of the number of particles and size distribution. These values remained stable during the first two minutes of nebulization

To test each mask in triplicate, we cut three circular pieces, 25 mm in diameter, from the mask and placed them in the filter holders. For each experiment, we first turned on the three pumps and then the nebulizer. After 2 min, we turned off the nebulizer. We allowed the pumps to run for an additional 2 min to remove most of the remaining aerosols from the chamber. We then opened the chamber and immediately transferred the mask pieces into sterile Petri dishes. We incubated the mask pieces at 28 °C and 80% RH, similar conditions that a mask worn by humans would experience, for 1 h. We attained the specified condition utilizing a CO_2 incubator while continuously monitoring temperature and humidity (Onset HOBO UX100-011A). We chose this condition based on a study of exhaled breath (25) and our own observations while wearing masks, using the same logger. For comparison, we also prepared samples at time zero following the same contamination protocol, with no incubation. This took place while the first set of samples was incubating for 1 h. The timing was such that we eluted both 1 h and time-zero samples simultaneously. To minimize cross-contamination, we cleaned the nebulizer and wiped the chamber with 70% ethanol between each experiment. We cleaned the support screens in the filter holders—these were in direct contact with the masks—with bleach and then 70% ethanol. Sample blanks of all masks, mounted in the filter holders and not exposed to virus, tested negative.

Skin Transfer Experiment

We prepared VITRO-SKIN (IMS Division of Florida Skincare Testing Inc.), which we refer to as "artificial skin", following the manufacturer's instructions. In short, we cut the artificial skin into 25 mm circular pieces and sterilized them with 70% ethanol. These pieces were then hydrated in a sealed, sterilized chamber with 15% glycerin in deionized water for 16–24 hours. (26) After hydration, each piece of artificial skin was aligned on top of a piece of contaminated mask without incubation. The topography side of the skin faced down, in contact with the outer layer of the mask. We placed 900 g of weights on the skin, generating a contact force of ~9 N and a pressure of 0.18 kg/cm^2. The contact lasted 10 s. The selected contact pressure and duration aimed to mimic people touching their masks. (27) The temperature was 22–23 °C and RH was ~30% during contact. We also pipetted 10 1 μL droplets of the SARS-CoV-2 stock on the skin and recovered the virus to test for inhibition effects. Mask pieces and artificial skin pieces were subjected to elution immediately after contact. We tested a blank skin piece that was hydrated but not in contact with the contaminated masks, and it was negative.

Mask and Skin Elution, Plaque Assay, and RT-qPCR

Environmental Science & Technology

for 1 min at 25 Hz. To estimate elution efficiency, we pipetted 10 1 μL droplets containing SARS-CoV-2 in saliva at a titer of $10^{5.0}$ PFU/mL onto the masks and then eluted them. We conducted this experiment in triplicate, and additional details can be found in the SI. After elution, we immediately transferred the eluates into a −80 °C freezer to preserve the virus for plaque assay and RNA extraction. (29) The elution efficiencies of the masks and artificial skin can be found in the SI.

We determined the amount of infectious virus recovered from each piece by plaque assay. We added 200 μL of the sample to each well with fully confluent Vero cells on a 6-well plate. We incubated the plates at 37 °C for 1 h and then overlaid 2 mL agarose medium comprising 0.8% agarose (SeaKem LE Agarose) and Ye-Lah medium (30) to each well, followed by incubation for 1 day at 37 °C. Then, we added the second 2 mL agarose overlay with additional 3% neutral red (1:300 solution, MP Biomedicals). A day later, we counted the plaques. As a positive control, we inoculated the Vero cells with six 10-fold dilutions of the SARS-CoV-2 stock. The lowest dilution was negative and served as the negative control. (24) We assigned 1 plaque to the largest dilution at which we did not observe plaque formation. The limit of detection (LOD) of the assay was 10 plaque-forming units (PFU) per piece, and we assigned this value to the results that were below the LOD when calculating statistics.

To extract and quantify RNA gene copies in the eluates, we used the Qiagen QIAamp Viral RNA Mini kit (Qiagen, Hilden, Germany) according to the manufacturer's protocol. The elution volume was 60 μL. Prior to qPCR, the extracts were stored at −80 °C. We quantified RNA by RT-qPCR using the 2019-nCoV RUO primer/probe kit (10006713, IDT, Coralville, IA) targeting the N1 gene (sequences in the SI) and the BioRad iTaq Universal Probes One-Step kit (BioRad, Hercules, CA). (31) We used synthetic SARS-CoV-2 RNA (NR-52358, BEI Resources, Manassas, VA) as standards (Figure S6). (32) Each plate contained duplicates of standard points, samples, and no-template controls. The LOD was 10 gene copies/piece based on the gene copy number at 40 cycles. More details can be found in the SI.

Statistics

We used the Student's *t*-test to compare samples at two time points: time zero and 1 h. These samples were generated using the same methods and differed only in the duration of incubation, so we assumed equal variance between the two sample types and equal distributions. The Student's *t*-test remains robust under various simulated conditions, including small sample size ($n \leq 3$), unequal variance, and different distributions. (33)

Environmental Science & Technology

Determination of the survival of aerosolized SARS-CoV-2 on masks depends on the ability of the mask to trap virus from the air and the efficiency of the elution method to transfer virus from the mask into liquid for subsequent analysis. The filtration efficiencies of masks tested in this study, at the most penetrating particle size, were >95% for the N95, 75% for the nylon/spandex mask, 60% for the surgical mask, and <50% for the cloth masks (including cotton knit, cotton poplin, and polyester). The average elution efficiencies of five of the masks ranged from 50 to 120% with large standard deviations, in the order of polyester > surgical > nylon/spandex > N95 > cotton knit (Figure S4); these values were not significantly different from 100% ($p > 0.05$), except for the cotton knit mask ($p = 0.01$). The elution efficiency of the cotton poplin mask was markedly lower, only 2%. The elution efficiency of the artificial skin was ~140% but not significantly different from 100% (Figure S5).

We also analyzed the surface roughness and hydrophobicity of the materials (Table 2) because these parameters have been shown to be related to the transfer of microbes from surfaces to skin. (27) The order of masks from smoothest to roughest was cotton poplin, surgical, nylon/spandex, N95 and polyester (same), and cotton knit (Table 2). We quantified hydrophobicity in terms of contact angle for hydrophobic materials and absorption time for hydrophilic ones. The order of masks from most hydrophobic to most hydrophilic was polyester, surgical, N95, nylon/spandex, cotton poplin, and cotton knit (Table 2).

SARS-CoV-2 Survival on Masks

Figure 2 shows the N1-domain gene copies and virus titer on 25 mm circular pieces of the masks at time zero and after 1 h at 28 °C and 80% RH, conditions intended to simulate those experienced by a mask while worn. We found the highest number of gene copies (5.4 $\log_{10}$-gene copies/piece) on the N95 respirator and the nylon/spandex mask and the lowest number (4.0 $\log_{10}$-gene copies/piece) on the cotton poplin mask (Figure 2a). The other masks were similar in terms of RNA recovery, ranging from 4.7 to 5.2 $\log_{10}$-gene copies/piece. The differences between time-zero samples and samples after 1 h incubation were within 0.4 $\log_{10}$-gene copies/piece across all samples. The number of gene copies recovered was positively correlated with filtration efficiency ($R^2 = 0.70$, $p < 0.05$) and elution efficiency ($R^2 = 0.10$, $p < 0.05$). The size distribution of virions in particles is unknown, so we did not have any expectations about the relationship with filtration efficiency, which varies by particle size. We expected that higher elution efficiency would result in greater recovery of virus from the masks. For example, the fewest gene copies were recovered from cotton poplin due to the combined effect of low filtration efficiency (<50%) and low elution efficiency (2%).

elution efficiency. Additionally, for this mask, the number of gene copies recovered after 1 h was greater than at time zero (4.3 vs 4.0 $\log_{10}$-gene copies/piece), possibly due to run-to-run variability of up to 50% in the amount of virus aerosolized. This uncertainty is addressed in a discussion of limitations, below.

Figure 2

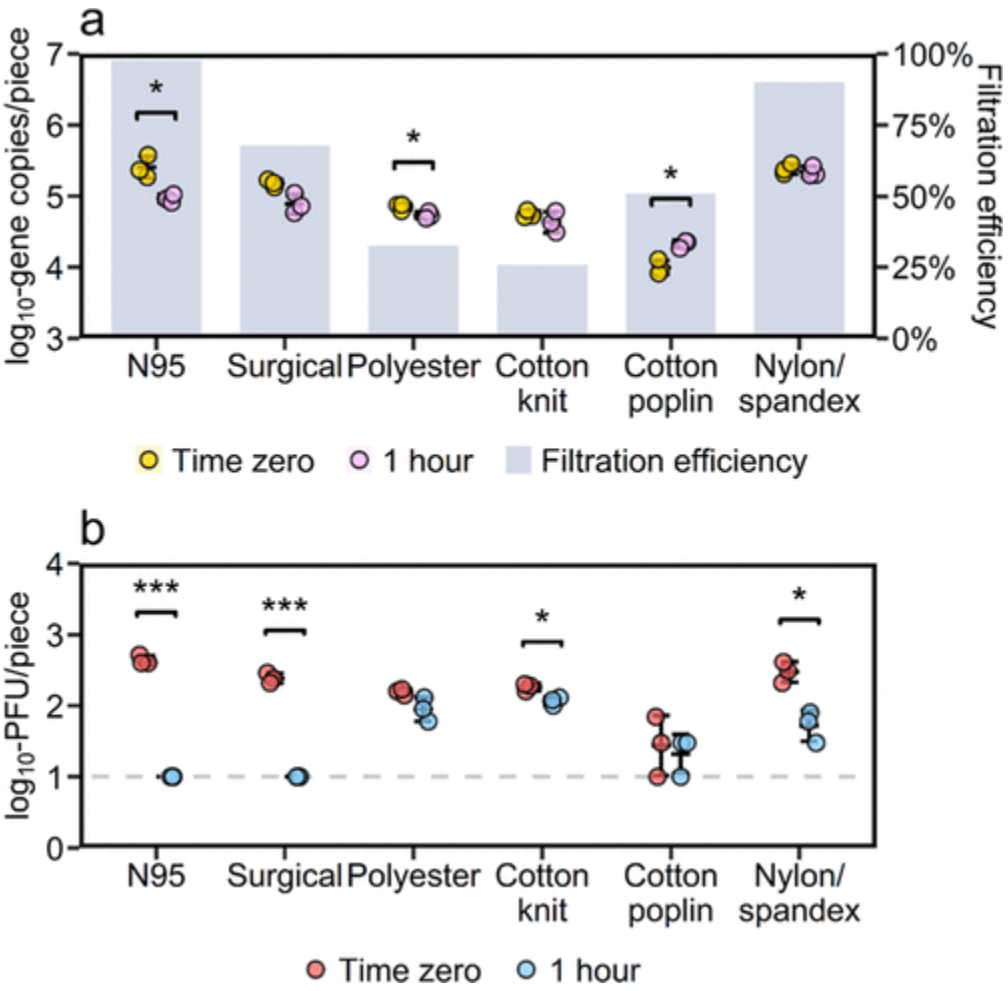

Figure 2. (a) Log_{10} N1-domain gene copies of SARS-CoV-2 on 25 mm circular mask pieces at time zero and after 1 h of incubation at 28 °C and 80% RH. (b) Virus titer on mask pieces at time zero and after 1 h in $\log_{10}$ plaque-forming unit (PFU)/piece. Error bars represent mean ± standard deviation. * $p < 0.05$ and *** $p < 0.001$. The gray dashed line represents the limit of detection (LOD).

We also recovered infectious virus from all mask pieces at time zero, and the virus titer was correlated with the number of gene copies (Figure 2b). The amount of infectious virus

polyester, cotton knit, and cotton poplin was minimal, 0.2, 0.1, and 0.1 $\log_{10}$-PFU/piece, respectively. Reduction was intermediate, 0.7 $\log_{10}$-PFU/piece, on the nylon/spandex mask.

To remove the dependence on the amount of virus aerosolized in each experiment, filtration efficiency, and elution efficiency, we calculated the ratio of gene copies to PFU for each mask and each time point (Figure 3). The initial ratio was between 2 and 3 $\log_{10}$ for all masks. An increase in this ratio indicates a decrease in infectious virus for a given number of gene copies. After 1 h, the ratios for the N95 respirator, surgical mask, and nylon/spandex mask increased, indicating decay of infectious virus while RNA levels remained stable. There was no significant difference in the ratios before and after incubation on the polyester, cotton knit, and cotton poplin masks.

Figure 3

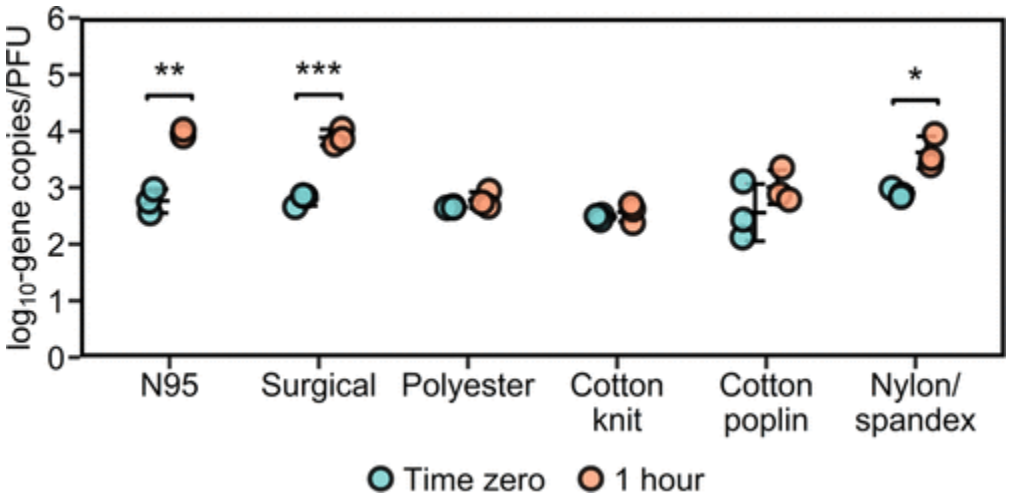

Figure 3. Log_{10} of the ratio of gene copies to plaque-forming units (PFU) at time zero and after 1 h of incubation at 28 °C and 80% RH. Error bars represent mean ± standard deviation. * $p < 0.05$; ** $p < 0.01$; *** $p < 0.001$.

Transfer of Aerosolized SARS-CoV-2 from Masks to Artificial Skin

We also explored the transfer of aerosolized SARS-CoV-2 from masks, without an incubation period, to artificial skin after 10 s of contact at a pressure of 0.18 kg/cm^2 (Figure 4). In this set of experiments, we detected similar RNA levels on the masks, 4–6 $\log_{10}$ gene copies/piece, as in the experiment on virus survival (Figure 2a). The amount transferred to and recovered from artificial skin was considerably lower, <3 $\log_{10}$-gene copies/piece, for all masks (Figure 4a); RNA was not detected on the skin that contacted the surgical mask. We

transferred from the masks to the skin, or any virus that was transferred lost infectivity during the process. In the case of the polyester mask, SARS-CoV-2 RNA was recovered but no infectious virus was found on either the mask or the skin.

Figure 4

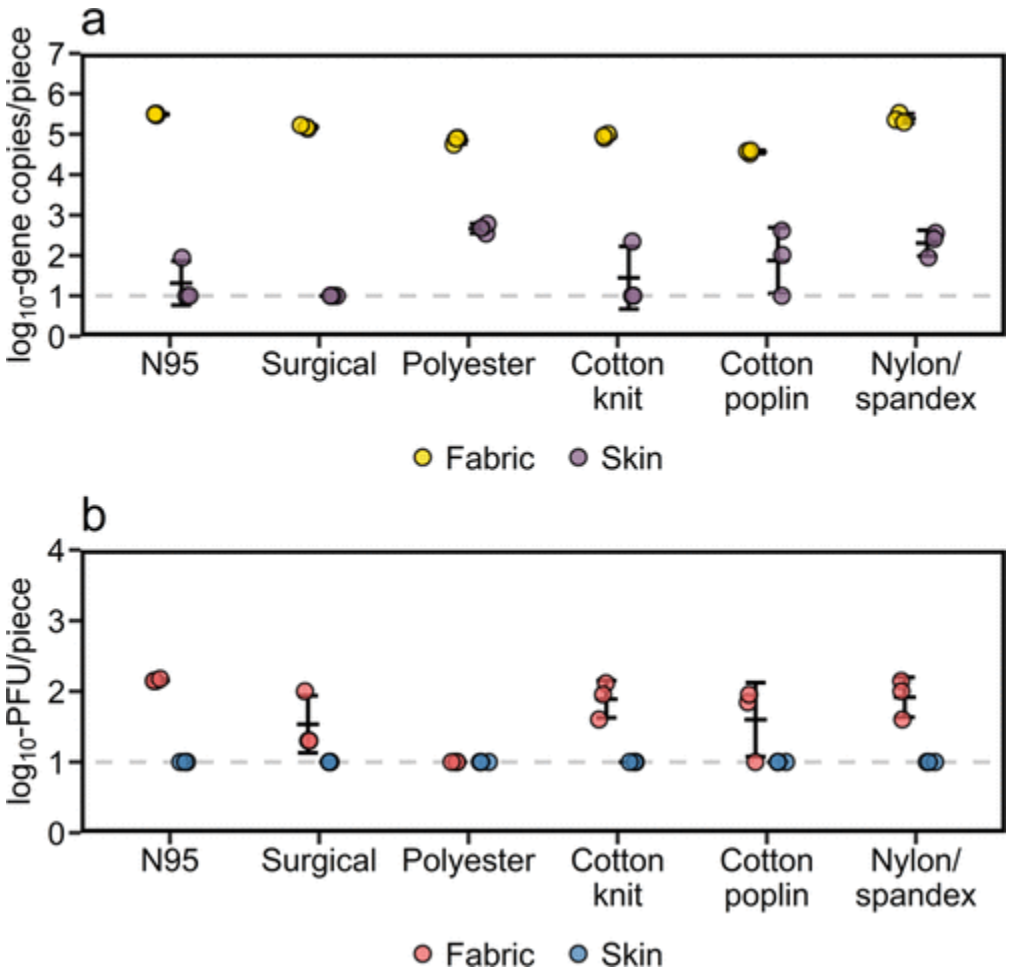

Figure 4. (a) Log_{10} N1-domain gene copies of SARS-CoV-2 on 25 mm circular mask pieces and artificial skin pressed against them for 10 s at a pressure of 0.18 kg/cm^2. (b) Virus titer on masks and artificial skin, in log_{10} plaque-forming unit (PFU)/piece. Error bars represent mean ± standard deviation. The gray dashed lines represent the limit of detection (LOD).

Discussion

Jump To

Comparisons among Studies of SARS-CoV-2 Survival on Surfaces

and surgical mask, aerosolized SARS-CoV-2 decayed to undetectable levels in terms of infectivity within 1 h. This is much shorter than the reported survival of SARS-CoV-2, applied in large droplets, on surgical masks for 4–7 days (8,11) and on N95s for several days. (10,13) In contrast, we observed no significant loss of infectivity after 1 h on a polyester mask, as opposed to a study in which SARS-CoV-2 in droplets decayed by 4 $\log_{10}$ on a polyester t-shirt within 1 h. (15) For cotton knit and cotton poplin, previous studies showed that SARS-CoV-2 in droplets exhibited 2–4 $\log_{10}$ decay in infectivity in 1 h, (10,11,15) whereas we observed <0.5 $\log_{10}$ decay of aerosolized SARS-CoV-2 on both cotton knit and cotton poplin masks.

The different method of contamination may have contributed to the contrast in results between studies. N95s and surgical masks typically consist of an outer layer, one or more middle layers of filter media, and an inner layer for comfort against the skin. Virus applied in large droplets may sit on the outer surface of the mask, depending on the material's hydrophobicity, and is subject to an extended evaporation process that does not occur with aerosols. Virus in aerosols is carried by air flow through the mask and may deposit at varying depths of the material. For masks constructed of layers of different materials, we expect most aerosols to be trapped in the middle filter layer(s), where they are less accessible to touch. The fate of virus on a mask could depend on the layer on which the virus is deposited.

Initial viral load may also affect persistence. In prior studies of SARS-CoV-2 stability, the lowest titer applied to a surface was 5×10^4 tissue culture infectious dose ($TCID_{50}$). (13) Here, we applied a similar amount of virus (~10^4 PFU) in aerosols to each mask piece, based on the amount of virus aerosolized (1 mL of suspension containing 10^5 PFU/mL), the amount pulled through each piece (1/3 each), and the material filtration efficiency (20–100%). SARS-CoV-2 concentrations on the order of 10 $TCID_{50}$ per liter of air have been detected in a patient room in a hospital, (34) so it would take ~100 min to load a high-quality mask with the amount of virus used in this study if we assume an inhalation rate of 10 L/min, and this load would be distributed over a larger area of the mask than the 25 mm circular pieces used here. We expect members of the public to encounter less virus in the air typically, so their masks would be less contaminated than in our experiments, and virus would likely decay at a rate faster than it accumulates on the mask. Despite the lack of evidence of transfer of infectious virus in our experiments, it is still possible that transient exposure to a high concentration of aerosolized virus followed by touching of the mask within minutes could lead to the transfer of infectious virus to fingers or another surface.

Other factors might also contribute to discrepancies in results between studies. Previous experiments were conducted under different environmental conditions (e.g., temperature and

Environmental Science & Technology

on the water content in virus-laden aerosols than hydrophobic fibers and may thus affect the factors listed above.

Potential Factors That Influence the Transfer from Masks to Skin

We recovered RNA, but no detectable infectious virus, from artificial skin that was in contact with the masks. We expect that most viruses were trapped in the middle layer of the masks, except for the two cotton masks, which lacked a special filter layer. If this is the case, then the chances of the skin coming into direct contact with viruses would be low. A low elution efficiency would also contribute to low probability of viruses being removed from the masks and transferred to other surfaces.

In previous studies in which SARS-CoV-2 or other viruses were applied in droplets to surfaces, the transfer efficiency of infectious virus to skin ranged from 2 to 80%. (19,20,27) Numerous factors could contribute to the large variability in results. A recent study showed that a decrease in surface roughness resulted in an increase in transfer efficiency from metal to skin. (27) However, such a trend was not evident in our study. The transfer efficiency of viral RNA was highest for the polyester mask, which had the second highest surface roughness, whereas it was lowest for the surgical mask, which had the second lowest roughness. This may be, in part, because we applied virus to the materials in the form of aerosols for the transfer experiment. The previous study also found that a higher contact pressure, rubbing, and multiple contacts resulted in a higher transfer efficiency. (27)

Humidity may also affect transfer of virus between surfaces. Another study reported that the transfer efficiency of deposited saliva aerosols from solid surfaces to artificial fingerpads increased from ~0 to ~60% when RH increased from 20 to 80%. (40) The low transfer efficiency in our study may be due, in part, to the low RH of 30% in the biosafety cabinet used for experiments, even though both artificial skin and masks were only exposed to this environment for 10 s. We might have observed a higher transfer efficiency if we had used a higher RH. The influence of RH on transfer efficiency is likely due to its regulation of the evaporation of aerosols and droplets and surface forces, but a mechanistic explanation is still unknown.

Material Effects

We found that the textile structure and treatment strongly affected the elution efficiency, even if the material was the same otherwise (Table 2 and Figures 2a,b and S4). For example, the elution efficiency was one order of magnitude lower for cotton poplin than for cotton knit. We

hydrophobicity of the masks, as indicated in Table 2 and Figure S4. In a study of decontamination methods for respirators, virus applied to the surface in large droplets (30 μL) survived better on a hydrophobic surface, on which a thick residue of nonvolatile solutes from saliva remained. (41) We did not observe a correlation between virus survival and hydrophobicity, perhaps because the aerosols had lost most water content before they were captured by the masks, (35,42) reducing the impact of hydrophobicity.

Limitations and Conclusions

There are several limitations to this study. We conducted three technical replicates and were not able to conduct multiple independent experiments due to the challenges of working with aerosolized SARS-CoV-2 in a BSL-3 laboratory. We believe the use of saliva as the suspending medium is more realistic compared to culture media, as used in most other studies, but it still differs from airway surface liquid, which may be more relevant for small aerosols that originate in the lower respiratory tract. In addition, run-to-run differences in aerosols generated by the nebulizer might have contributed to uncertainties in results (Figure S2). While we ran experiments at a single temperature and RH, future studies should consider varying these parameters, particularly for investigating the transfer of virus from fomites to skin. Of note, our study focused on virus-laden aerosols captured by masks. Any virus that penetrates through a mask, due to low filtration efficiency or poor fit, might otherwise lead to exposure through inhalation.

To conclude, the risk of fomite transmission via contamination of masks by SARS-CoV-2 in aerosols is likely to be very low, lower than suggested by experiments involving large droplets, and certainly lower than would occur if a person did not wear a mask and were fully exposed through inhalation. The influence of environmental factors, suspending media, and textile structure on the survival and transfer of SARS-CoV-2 also requires further investigation. We continue to recommend high-quality, well-fitting masks as one of the most effective tools to reduce the risk of infection with SARS-CoV-2 and other emerging pathogens that are transmitted through the air.

Supporting Information

Jump To

The Supporting Information is available free of charge at https://pubs.acs.org/doi/10.1021/acs.est.3c01581.

- Summary of survival of SARS-CoV-2 droplets on fabrics from the literature (Table S1);

filtration efficiency as a function of particle size (Figure S3); elution efficiency of washed masks and artificial skin (Figures S4 and S5); and detailed description of RT-qPCR and standard curves (Figure S6) (PDF)

Stability of Aerosolized SARS-CoV-2 on Masks and Transfer to Skin

15 views | 0 shares | 0 downloads

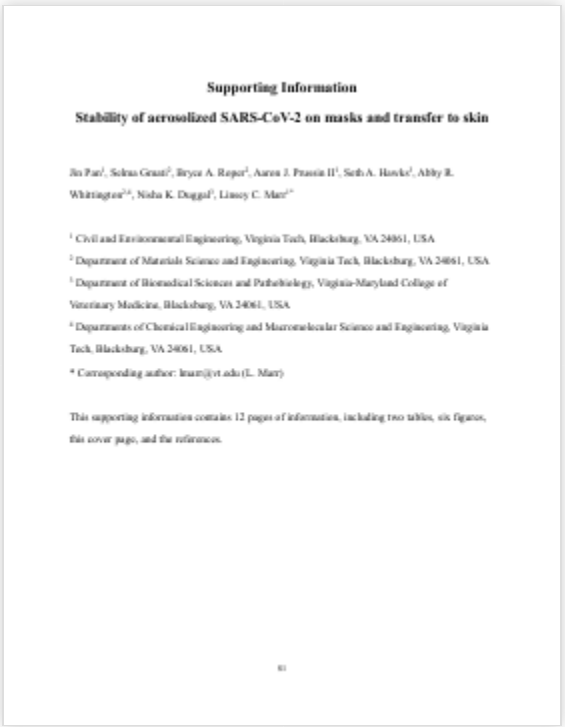

Supporting Information

Stability of aerosolized SARS-CoV-2 on masks and transfer to skin

Jin Pan[1], Selma Gurol[2], Bryce A. Reper[1], Aaron J. Prussin II[3], Seth A. Hawks[3], Abby R. Whittington[2,4], Nisha K. Duggal[3], Linsey C. Marr[1,*]

[1] Civil and Environmental Engineering, Virginia Tech, Blacksburg, VA 24061, USA
[2] Department of Materials Science and Engineering, Virginia Tech, Blacksburg, VA 24061, USA
[3] Department of Biomedical Sciences and Pathobiology, Virginia-Maryland College of Veterinary Medicine, Blacksburg, VA 24061, USA
[4] Departments of Chemical Engineering and Macromolecular Science and Engineering, Virginia Tech, Blacksburg, VA 24061, USA
* Corresponding author: lmarr@vt.edu (L. Marr)

This supporting information contains 12 pages of information, including two tables, six figures, this cover page, and the references.

S1

Expand

Terms & Conditions

obtained from ACS for other uses through requests via the RightsLink permission system: http://pubs.acs.org/page/copyright/permissions.html.

Author Information

Jump To

Corresponding Author

Linsey C. Marr - *Civil and Environmental Engineering, Virginia Tech, Blacksburg, Virginia 24061, United States*; https://orcid.org/0000-0003-3628-6891; Email: lmarr@vt.edu

Authors

Jin Pan - *Civil and Environmental Engineering, Virginia Tech, Blacksburg, Virginia 24061, United States*; https://orcid.org/0000-0001-8699-2394

Selma Gmati - *Department of Materials Science and Engineering, Virginia Tech, Blacksburg, Virginia 24061, United States*

Bryce A. Roper - *Department of Materials Science and Engineering, Virginia Tech, Blacksburg, Virginia 24061, United States*

Aaron J. Prussin - *Civil and Environmental Engineering, Virginia Tech, Blacksburg, Virginia 24061, United States*; https://orcid.org/0000-0002-9991-8537

Seth A. Hawks - *Department of Biomedical Sciences and Pathobiology, Virginia-Maryland College of Veterinary Medicine, Blacksburg, Virginia 24061, United States*

Abby R. Whittington - *Department of Materials Science and Engineering, Virginia Tech, Blacksburg, Virginia 24061, United States*; *Departments of Chemical Engineering and Macromolecular Science and Engineering, Virginia Tech, Blacksburg, Virginia 24061, United States*; https://orcid.org/0000-0001-7401-7209

Nisha K. Duggal - *Department of Biomedical Sciences and Pathobiology, Virginia-Maryland College of Veterinary Medicine, Blacksburg, Virginia 24061, United States*

Notes

The authors declare no competing financial interest.

Acknowledgments

Jump To

Virginia Tech's Center for Emerging, Zoonotic, and Arthropod-borne Pathogens, Fralin Life Sciences Institute, and Institute for Critical Technology and Applied Science provided support for this work. The authors thank Dr. Jennifer Van Mullekom, Director of the Statistical

Environmental Science & Technology

References

Jump To

This article references 42 other publications.

1. Dargahi, A.; Jeddi, F.; Ghobadi, H.; Vosoughi, M.; Karami, C.; Sarailoo, M.; Hadisi, A.; Mokhtari, S. A.; Haghighi, S. B.; Sadeghi, H.; Alighadri, M. Evaluation of masks' internal and external surfaces used by health care workers and patients in coronavirus-2 (SARS-CoV-2) wards. *Environ. Res.* **2021**, *196*, 110948
DOI: 10.1016/j.envres.2021.110948

| Google Scholar

2. Ruiz-Bastián, M.; Rodríguez-Tejedor, M.; Rivera-Núñez, M. A.; SARS-CoV-2 Working Group Detection of SARS-CoV-2 genomic RNA on surgical masks worn by patients: Proof of concept. *Enferm. Infecc. Microbiol. Clin. (Engl. Ed.)* **2021**, *39*, 528– 530, DOI: 10.1016/j.eimc.2020.12.004

| Google Scholar

3. Allen, J. G.; Marr, L. C. Recognizing and controlling airborne transmission of SARS-CoV-2 in indoor environments. *Indoor Air* **2020**, *30*, 557– 558, DOI: 10.1111/ina.12697

| Google Scholar

4. Morawska, L.; Tang, J. W.; Bahnfleth, W.; Bluyssen, P. M.; Boerstra, A.; Buonanno, G.; Cao, J.; Dancer, S.; Floto, A.; Franchimon, F.; Haworth, C.; Hogeling, J.; Isaxon, C.; Jimenez, J. L.; Kurnitski, J.; Li, Y.; Loomans, M.; Marks, G.; Marr, L. C.; Mazzarella, L.; Melikov, A. K.; Miller, S.; Milton, D. K.; Nazaroff, W.; Nielsen, P. V.; Noakes, C.; Peccia, J.; Querol, X.; Sekhar, C.; Seppänen, O.; Tanabe, S.-i.; Tellier, R.; Tham, K. W.; Wargocki, P.; Wierzbicka, A.; Yao, M. How can airborne transmission of COVID-19 indoors be minimised?. *Environ. Int.* **2020**, *142*, 105832
DOI: 10.1016/j.envint.2020.105832

| Google Scholar

5. Asadi, S.; Bouvier, N.; Wexler, A. S.; Ristenpart, W. D. The coronavirus pandemic and aerosols: Does COVID-19 transmit via expiratory particles?. *Aerosol Sci. Technol.* **2020**, *54*, 635– 638,
DOI: 10.1080/02786826.2020.1749229

based on the current evidence. *Aerosol Air Qual. Res.* **2020**, *20*, 911– 914, DOI: 10.4209/aaqr.2020.04.0158

| Google Scholar

7. Prather, K. A.; Wang, C. C.; Schooley, R. T. Reducing transmission of SARS-CoV-2. *Science* **2020**, *368*, 1422–1424, DOI: 10.1126/science.abc6197

| Google Scholar

8. Chin, A. W.; Chu, J. T.; Perera, M. R. Correspondence. Stability of SARS-CoV-2 in different environmental conditions. *Lancet Microbe* **2020**, *1*, 30003 DOI: 10.1016/S2666-5247(20)30003-3

| Google Scholar

9. van Doremalen, N.; Bushmaker, T.; Morris, D. H.; Holbrook, M. G.; Gamble, A.; Williamson, B. N.; Tamin, A.; Harcourt, J. L.; Thornburg, N. J.; Gerber, S. I.; Lloyd-Smith, J. O.; de Wit, E.; Munster, V. J. Aerosol and surface stability of SARS-CoV-2 as compared with SARS-CoV-1. *N. Engl. J. Med.* **2020**, *382*, 1564– 1567, DOI: 10.1056/NEJMc2004973

| Google Scholar

10. Kasloff, S. B.; Leung, A.; Strong, J. E.; Funk, D.; Cutts, T. Stability of SARS-CoV-2 on critical personal protective equipment. *Sci. Rep.* **2021**, *11*, 984 DOI: 10.1038/s41598-020-80098-3

| Google Scholar

11. Liu, Y.; Li, T.; Deng, Y.; Liu, S.; Zhang, D.; Li, H.; Wang, X.; Jia, L.; Han, J.; Bei, Z.; Li, L.; Li, J. Stability of SARS-CoV-2 on environmental surfaces and in human excreta. *J. Hosp. Infect.* **2021**, *107*, 105– 107, DOI: 10.1016/j.jhin.2020.10.021

| Google Scholar

13. Kwon, T.; Gaudreault, N. N.; Richt, J. A. Environmental stability of SARS-CoV-2 on different types of surfaces under indoor and seasonal climate conditions. *Pathogens* **2021**, *10*, 227, DOI: 10.3390/pathogens10020227

| Google Scholar

14. Harbourt, D. E.; Haddow, A. D.; Piper, A. E.; Bloomfield, H.; Kearney, B. J.; Fetterer, D.; Gibson, K.; Minogue, T. Modeling the stability of severe acute respiratory syndrome coronavirus 2 (SARS-CoV-2) on skin, currency, and clothing. *PLOS Neglected Trop. Dis.* **2020**, *14*, e0008831 DOI: 10.1371/journal.pntd.0008831

| Google Scholar

15. Paton, S.; Spencer, A.; Garratt, I.; Thompson, K.-A.; Dinesh, I.; Aranega-Bou, P.; Stevenson, D.; Clark, S.; Dunning, J.; Bennett, A.; Pottage, T. Persistence of severe acute respiratory syndrome coronavirus 2 (SARS-CoV-2) virus and viral RNA in relation to surface type and contamination concentration. *Appl. Environ. Microbiol.* **2021**, *87*, e00526-21, DOI: 10.1128/AEM.00526-21

| Google Scholar

16. Johnson, G. R.; Morawska, L.; Ristovski, Z. D.; Hargreaves, M.; Mengersen, K.; Chao, C. Y. H.; Wan, M. P.; Li, Y.; Xie, X.; Katoshevski, D.; Corbett, S. Modality of human expired aerosol size distributions. *J. Aerosol Sci.* **2011**, *42*, 839– 851, DOI: 10.1016/j.jaerosci.2011.07.009

| Google Scholar

17. Morawska, L.; Johnson, G. R.; Ristovski, Z. D.; Hargreaves, M.; Mengersen, K.; Corbett, S.; Chao, C. Y. H.; Li, Y.; Katoshevski, D. Size distribution and sites of origin of droplets expelled from the human respiratory tract during expiratory activities. *J. Aerosol Sci.* **2009**, *40*, 256– 269, DOI: 10.1016/j.jaerosci.2008.11.002

| Google Scholar

18. French, A. J.; Longest, A. K.; Pan, J.; Vikesland, P. J.; Duggal, N. K.; Marr, L. C.; Lakdawala, S. S. Environmental stability of enveloped viruses is impacted by initial volume and evaporation kinetics of droplets. *mBio* **2023**, *14*, e03452– 22, DOI: 10.1128/mbio.03452-22

19. Benzadiasab, S.; Chin, A. W. H.; Hosseini, M.; Poon, L. L. M.; Ducker, W. A. SARS-CoV-2 virus transfers to skin through contact with contaminated solids. *Sci. Rep.* **2021**, *11*, 22868 DOI: 10.1038/s41598-021-00843-0

| Google Scholar

20. Anderson, C. E.; Boehm, A. B. Transfer rate of enveloped and nonenveloped viruses between fingerpads and surfaces. *Appl. Environ. Microbiol.* **2021**, *87*, e01215-21, DOI: 10.1128/AEM.01215-21

| Google Scholar

21. Rusin, P.; Maxwell, S.; Gerba, C. Comparative surface-to-hand and fingertip-to-mouth transfer efficiency of gram-positive bacteria, gram-negative bacteria, and phage. *J. Appl. Microbiol.* **2002**, *93*, 585– 592, DOI: 10.1046/j.1365-2672.2002.01734.x

| Google Scholar

22. Hirose, R.; Ikegaya, H.; Naito, Y. Survival of SARS-CoV-2 and influenza virus on the human skin: Importance of hand hygiene in COVID-19 *Clin. Infect. Dis.* 2020.

Google Scholar

23. Pan, J.; Harb, C.; Leng, W.; Marr, L. C. Inward and outward effectiveness of cloth masks, a surgical mask, and a face shield. *Aerosol Sci. Technol.* **2021**, *55*, 718– 733, DOI: 10.1080/02786826.2021.1890687

| Google Scholar

24. Hawks, S. A.; Prussin, A. J.; Kuchinsky, S. C.; Pan, J.; Marr, L. C.; Duggal, N. K. Infectious SARS-CoV-2 Is Emitted in Aerosol Particles. *mBio* **2021**, *12*, e0252721 DOI: 10.1128/mBio.02527-21

| Google Scholar

25. Mansour, E.; Vishinkin, R.; Rihet, S.; Saliba, W.; Fish, F.; Sarfati, P.; Haick, H. Measurement of temperature and relative humidity in exhaled breath. *Sens. Actuators, B* **2020**, *304*, 127371 DOI: 10.1016/j.snb.2019.127371

| Google Scholar

27. Zhao, P.; Li, Y. Modeling and experimental validation of microbial transfer via surface touch. *Environ. Sci. Technol.* **2021**, *55*, 4148– 4161, DOI: 10.1021/acs.est.0c04678

| Google Scholar

28. Bunning, M. L.; Bowen, R. A.; Cropp, C. B.; Sullivan, K. G.; Davis, B. S.; Komar, N.; Godsey, M. S.; Baker, D.; Hettler, D. L.; Holmes, D. A.; Biggerstaff, B. J.; Mitchell, C. J. Experimental infection of horses with West Nile virus. *Emerging Infect. Dis.* **2002**, *8*, 380– 386, DOI: 10.3201/eid0804.010239

| Google Scholar

29. Gould, E. A. Methods for long-term virus preservation. *Mol. Biotechnol.* **1999**, *13*, 57– 66, DOI: 10.1385/MB:13:1:57

| Google Scholar

30. Poole-Smith, B. K.; Hemme, R. R.; Delorey, M.; Felix, G.; Gonzalez, A. L.; Amador, M.; Hunsperger, E. A.; Barrera, R. Comparison of vector competence of aedes mediovittatus and aedes aegypti for dengue virus: Implications for dengue control in the caribbean. *PLOS Neglected Trop. Dis.* **2015**, *9*, e0003462 DOI: 10.1371/journal.pntd.0003462

| Google Scholar

31. Lu, X.; Wang, L.; Sakthivel, S. K.; Whitaker, B.; Murray, J.; Kamili, S.; Lynch, B.; Malapati, L.; Burke, S. A.; Harcourt, J., et al. US CDC real-time reverse transcription PCR panel for detection of severe acute respiratory syndrome coronavirus 2. *Emerging Infect. Dis.* **2020**, *26*, 1654, DOI: 10.3201/eid2608.201246

| Google Scholar

| Google Scholar

33. De Winter, J. C. Using the student's t-test with extremely small sample sizes. *Pract. Assess., Res. Eval.* **2013**, *18*, 10, DOI: 10.7275/e4r6-dj05

| Google Scholar

34. Lednicky, J. A.; Lauzardo, M.; Fan, Z. H.; Jutla, A.; Tilly, T. B.; Gangwar, M.; Usmani, M.; Shankar, S. N.; Mohamed, K.; Eiguren-Fernandez, A.; Stephenson, C. J.; Alam, M. M.; Elbadry, M. A.; Loeb, J. C.; Subramaniam, K.; Waltzek, T. B.; Cherabuddi, K.; Morris, J. G., Jr.; Wu, C.-Y. Viable SARS-CoV-2 in the air of a hospital room with COVID-19 patients. *Int. J. Infect. Dis.* **2020**, *100*, 476– 482, DOI: 10.1016/j.ijid.2020.09.025

| Google Scholar

35. Oswin, H. P.; Haddrell, A. E.; Otero-Fernandez, M.; Mann, J. F. S.; Cogan, T. A.; Hilditch, T. G.; Tian, J.; Hardy, D. A.; Hill, D. J.; Finn, A.; Davidson, A. D.; Reid, J. P. The dynamics of SARS-CoV-2 infectivity with changes in aerosol microenvironment. *Proc. Natl. Acad. Sci. U.S.A.* **2022**, *119*, e2200109119 DOI: 10.1073/pnas.2200109119

| Google Scholar

36. Lin, K.; Schulte, C. R.; Marr, L. C. Survival of MS2 and Φ6 viruses in droplets as a function of relative humidity, pH, and salt, protein, and surfactant concentrations. *PLoS One* **2020**, *15*, e0243505 DOI: 10.1371/journal.pone.0243505

| Google Scholar

37. Zou, L.; Ruan, F.; Huang, M.; Liang, L.; Huang, H.; Hong, Z.; Yu, J.; Kang, M.; Song, Y.; Xia, J.; Guo, Q.; Song, T.; He, J.; Yen, H.-L.; Peiris, M.; Wu, J. SARS-CoV-2 viral load in upper respiratory specimens of infected patients. *N. Engl. J. Med.* **2020**, *382*, 1177– 1179, DOI: 10.1056/NEJMc2001737

| Google Scholar

38. Huynh, E.; Olinger, A.; Woolley, D.; Kohli Ravleen, K.; Choczynski Jack, M.; Davies James, F.; Lin, K.; Marr Linsey, C.; Davis Ryan, D. Evidence for a semisolid phase state of aerosols and droplets relevant to the airborne and surface survival of pathogens. *Proc. Natl. Acad. Sci. U.S.A.* **2022**, *119*, e2109750119

39. Wei, H.; Vejerano Eric, P.; Leng, W.; Huang, Q.; Willner Marjorie, R.; Marr Linsey, C.; Vikesland Peter, J. Aerosol microdroplets exhibit a stable pH gradient. *Proc. Natl. Acad. Sci. U.S.A.* **2018**, *115*, 7272– 7277, DOI: 10.1073/pnas.1720488115

| Google Scholar

40. Walker, M. D.; Vincent, J. C.; Benson, L.; Stone, C. A.; Harris, G.; Ambler, R. E.; Watts, P.; Slatter, T.; López-García, M.; King, M.-F.; Noakes, C. J.; Thomas, R. J. Effect of relative humidity on transfer of aerosol-deposited artificial and human saliva from surfaces to artificial finger-pads. *Viruses* **2022**, *14*, 1048, DOI: 10.3390/v14051048

| Google Scholar

41. Oh, C.; Araud, E.; Puthussery, J. V.; Bai, H.; Clark, G. G.; Wang, L.; Verma, V.; Nguyen, T. H. Dry heat as a decontamination method for N95 respirator reuse. *Environ. Sci. Technol. Lett.* **2020**, *7*, 677– 682, DOI: 10.1021/acs.estlett.0c00534

| Google Scholar

42. Walker, J. S.; Archer, J.; Gregson, F. K. A.; Michel, S. E. S.; Bzdek, B. R.; Reid, J. P. Accurate representations of the microphysical processes occurring during the transport of exhaled aerosols and droplets. *ACS Cent. Sci.* **2021**, *7*, 200– 209, DOI: 10.1021/acscentsci.0c01522

| Google Scholar

Cited By

Jump To

This article is cited by 2 publications.

1. Trisha Greenhalgh, C. Raina MacIntyre, Michael G. Baker, Shovon Bhattacharjee, Abrar A. Chughtai, David Fisman, Mohana Kunasekaran, Amanda Kvalsvig, Deborah Lupton, Matt Oliver, Essa Tawfiq, Mark Ungrin, Joe Vipond, , Linsey Marr. Masks and respirators for prevention of respiratory infections: a state of the science review. *Clinical Microbiology Reviews* 2024, *37* (2) https://doi.org/10.1128/cmr.00124-23

2. Alexander S Rabin, Linsey C Marr, Henry M Blumberg. Doff Thy Gown—Shedding Contact Precautions for

Environmental Science & Technology

Download PDF

Partners

Washington, DC 20036
Copyright © 2024
American Chemical Society